A left bundle branch block activation sequence and ventricular pacing influence voltage amplitudes: an in vivo and in silico study

Uyên Châu Nguyên, Mark Potse, Kevin Vernooy, Masih Mafi-Rad, Jordi Heijman, Maria Luce Caputo, Giulio Conte, François Regoli, Rolf Krause, Tiziano Moccetti, et al.

A left bundle branch block activation sequence and ventricular pacing influences voltage amplitudes: an in vivo and in silico study

Uyên Châu Nguyên, MD, MSc,[1,2] Mark Potse, PhD,[3,4,5] Kevin Vernooy, MD, PhD,[2,6] Masih Mafi-Rad, MD, PhD,[2] Jordi Heijman, PhD,[2] Maria Luce Caputo MD,[7] Giulio Conte MD, PhD,[7] François Regoli MD, PhD,[7] Rolf Krause, PhD,[8] Tiziano Moccetti MD,[7] Angelo Auricchio, MD, PhD,[7,8] Frits W. Prinzen, PhD,[1] Francesco Maffessanti, PhD[8]

[1] Department of Physiology, Cardiovascular Research Institute Maastricht (CARIM), Maastricht University Medical Center (MUMC+), Maastricht, the Netherlands

[2] Department of Cardiology, CARIM, MUMC+, Maastricht, the Netherlands

[3] CARMEN Research Team, Inria Bordeaux Sud-Ouest, F-33400 Talence, France

[4] Université de Bordeaux, IMB, UMR 5251, F-33400 Talence, France

[5] IHU Liryc, Electrophysiology and Heart Modeling Institute, foundation Bordeaux Université, F-33600 Pessac-Bordeaux, France

[6] Department of Cardiology, Radboud University Medical Center, Nijmegen, the Netherlands

[7] Department of Cardiology, Fondazione Cardiocentro Ticino, Lugano, Switzerland

[8] Center for Computational Medicine in Cardiology (CCMC), Institute of Computational Science, Università della Svizzera italiana, Lugano, Switzerland

Correspondence to:

Uyên Châu Nguyên, Department of Physiology, Cardiovascular Research Institute Maastricht, PO Box 616, 6200 MD, Maastricht, the Netherlands. Tel: +31-43-3881200; fax: +31-43-3884166. Email: u.nguyen@maastrichtuniversity.nl

Abstract

Aim: The aim of this study was to investigate the influence of activation sequence on voltage amplitudes by evaluating regional voltage differences during a left bundle branch block (LBBB) activation sequence versus a normal synchronous activation sequence and by evaluating pacing-induced voltage differences.

Methods: 21 patients and 3 computer models without scar were studied. Regional voltage amplitudes were evaluated in 9 LBBB patients who underwent endocardial electro-anatomic mapping (EAM). Pacing-induced voltage differences were evaluated in 12 patients who underwent epicardial EAM during intrinsic rhythm and right ventricular (RV) pacing. Three computer models customized for LBBB patients were created. Changes in voltage amplitudes after an LBBB (intrinsic), a normal synchronous, a right ventricular (RV) pacing, and a left ventricular (LV) pacing activation sequence were assessed in the computer models.

Results: Unipolar voltage amplitudes in patients were ~4.5 mV (4.4-4.7 mV, ~33%) lower in the septum compared to other segments. A normal synchronous activation sequence in the computer models normalized voltage amplitudes in the septum. Pacing-induced differences were larger in electrograms with higher voltage amplitudes during intrinsic rhythm and furthermore larger and more variable at the epicardium (mean absolute difference: 3.6-6.2 mV, 40-53% of intrinsic value; IQR differences: 53-63% of intrinsic value) compared to the endocardium (mean absolute difference: 3.3-3.8 mV, 28-30% of intrinsic value; IQR differences: 37-40% of intrinsic value).

Conclusion: In patients and computer models without scar, lower septal unipolar voltage amplitudes are exclusively associated with an LBBB activation sequence. Pacing substantially affects voltage amplitudes, particularly at the epicardium.

Keywords

Voltage amplitude; intra-cardiac electrogram; heart failure; left bundle branch block; activation sequence; computer models; anisotropy.

Condensed abstract

This study investigates the influence of activation sequence on voltage amplitudes. In patients and computer models without scar, lower unipolar voltage amplitudes in the septum are exclusively associated with a left bundle branch block activation sequence. Ventricular pacing furthermore substantially affects voltage amplitudes with average changes of half of intrinsic value.

What's new?

- This study investigates the influence of activation sequence on voltage amplitudes in patients and provides possible explanations for these changes using computer modeling.
- In patients and computer models without scar, lower unipolar voltage amplitudes in the septum are exclusively associated with a left bundle branch block activation sequence.
- Ventricular pacing substantially affects voltage amplitudes in both patients and computer models with changes of half of intrinsic value.

Introduction

Low voltage amplitudes from electro-anatomic mapping (EAM) are widely considered as a reference tool for scar delineation[1] and have been associated with scar on delayed enhancement cardiac magnetic resonance imaging (DE-CMR).[2] Nevertheless, significant overlap in voltage amplitudes between scar and normal myocardium and substantial inter-patient differences[3-5] limit the validity of distinct voltage cut-off values to identify scar.[6]

These data suggest that additional factors may affect the voltage amplitudes.[7] Substantial differences in characterization of scar by low-voltage areas between intrinsic rhythm and ventricular pacing were recently reported,[8] indicating that the activation sequence influences voltage amplitudes.

Besides during pacing, an abnormal activation sequence can also occur in the presence of inter- and intraventricular conduction disturbances. For instance, a left bundle branch block (LBBB) activation sequence is characterized by a slow impulse conduction originating from the right ventricular (RV) free wall gradually propagating to the left ventricular (LV) free wall.[9] The influence of an LBBB activation sequence on voltage amplitudes has not been elucidated before.

The aim of this study was to investigate the influence of activation sequence on voltage amplitudes at the endocardium and epicardium in patients with heart failure (HF). In order to improve mechanistic understanding of this influence, regional voltage amplitudes in LBBB patients and computer models without scar were studied. To compare voltage amplitudes during an LBBB activation sequence and a normal synchronous activation sequence, which was not possible in patients, we used highly realistic computer simulations with three customized models of LBBB patients. Additionally, voltage differences induced by ventricular pacing were evaluated both in patients and in computer models.

Methods

Patient population

Patients referred for a CRT device implantation who underwent LV endocardial EAM[3] or epicardial (coronary venous) EAM[10] were included in this study. To minimize other sources of variation in voltage amplitudes only patients without scar were included.

The Comitato Etico del Canton Ticino in Lugano and the Medical Ethics Committee of Maastricht University Medical Center approved the study protocol.

Electro-anatomic mapping

Patients underwent either endocardial or epicardial EAM. Voltage amplitudes were computed peak-to-peak and activation times were defined as the duration between onset of QRS-complex on the surface electrocardiogram (ECG) to the moment of steepest downslope on the intra-cardiac electrogram.

Endocardial EAM was performed during intrinsic rhythm using the NOGA XP Cardiac Navigation System (Biosense Webster, Irvine, CA, USA) as previously described.[11] Unipolar and bipolar electrograms and catheter tip trajectories in 3D space were simultaneously recorded at the entire LV endocardium (bandpass filter: 1–240 Hz). Care was taken to cover the whole LV cavity until NOGA mapped volume was close to the CMR measured volume and the system automatically discards points with insufficient wall contact. All acquired signals were temporally aligned using the simultaneously recorded surface ECG.

Epicardial EAM was performed during intrinsic rhythm and RV pacing using EnSite NavX (Abbott, Chicago, Ill, USA) as described previously.[10] A guidewire permitting unipolar sensing and pacing was inserted into the coronary sinus and manipulated to all accessible tributaries, creating an anatomic 3D map of the coronary veins while simultaneously recording electrograms (bandpass filter: 2–300 Hz) and a surface ECG. RV pacing was performed with the implanted RV lead at 10 beats per minute above the intrinsic heart rate in DDD-mode with a short AV-delay to ensure full ventricular capture. Electrograms with poor signal indicating poor contact were manually discarded during the procedure.

Computer models

Three patient-specific computer models were created.[12] Each model geometry was based on CMR imaging of the heart, lungs, and torso surface. The electrophysiological properties of the models were personalized based on the patients' endocardial EAM and 12-lead ECG acquired during sinus rhythm, and geometries were personalized using the CMR-derived heart-lungs-torso anatomies.[12] Simulations were performed with the Propag-5 software[13] on 2304 cores of the Bullx cluster "Curie" (TGCC, CEA, France). A ventricular model with a 0.2-mm resolution

and a torso model with 1-mm resolution were used. Propagating electrical activity was simulated based on ionic transmembrane currents according to a monodomain reaction-diffusion equation.[14] The Ten Tusscher-Noble-Noble-Panfilov model of the human ventricular cardiomyocyte[15] was used to compute the ionic currents. Computed transmembrane currents were injected at 1-ms intervals in the torso model and the bidomain equation was solved for the electrical potential throughout the torso, from which electrograms at the LV endocardium and epicardium were extracted.[16] A normal activation sequence (synchronous activation) was simulated by inducing multiple breakthroughs in a thin, rapidly conducting endocardial layer mimicking the Purkinje network activation. A RV pacing simulation was created by single-point pacing in the RV endocardium apex, while a LV pacing simulation was created by single-point pacing in the LV epicardium. Similar to clinical data, unipolar voltage amplitudes were computed peak-to-peak and activation times were quantified as the duration between onset of the QRS-complex and the moment of steepest downslope on the intra-cardiac electrogram.

Data analyses

Data were expressed as mean±standard deviation (SD) or median and interquartile (IQR) range. Analyses were performed in MATLAB 2016b (Mathworks, Natick, MA, USA). Non-parametric test approaches were used for patient data analyses. Statistical significance was not evaluated in the simulated data, as it has been argued that statistical comparisons of computer models are inappropriate.[17] Absolute values were therefore used to describe the simulated data instead. Regional voltage differences in patients and computer models were compared by subdividing the LV into four segments: anterior, lateral, inferior, and septal. Intrinsic voltage amplitudes were compared between segments and for all patients with endocardial EAM using Kruskal Wallis tests.

Pacing-induced voltage changes were evaluated in patients with epicardial EAM and computer models by assessing differences as absolute and relative (percentage of intrinsic value) numbers. For the epicardial EAM patient data, paired comparisons were carried out by matching every electrogram during intrinsic rhythm with the nearest electrogram obtained during RV pacing under the condition that the Euclidean distance between the two electrograms was <15 mm. In the computer models, paired comparisons were performed by comparing electrograms during

different activation sequences from the same vertex in 3D space. Relative differences between every paired electrogram (depicted in mV or percentage of intrinsic value) were computed as:

$$\text{Difference [mV]} = \frac{\text{Intrinsic} - \text{paced}}{\text{Intrinsic}}$$

or

$$\text{Difference [\% intrinsic]} = \frac{\text{Intrinsic} - \text{paced}}{\text{Intrinsic}} * 100\%$$

Absolute differences were computed similarly as:

$$\text{Difference [mV]} = \frac{\text{abs(Intrinsic} - \text{paced)}}{\text{Intrinsic}}$$

or

$$\text{Absolute difference [\% intrinsic]} = \frac{\text{abs(Intrinsic} - \text{paced)}}{\text{Intrinsic}} * 100\%$$

Bland-Altman analyses were carried out to evaluate the agreement between voltage amplitudes during intrinsic rhythm and pacing.

Results

Study population

A total of 21 patients and 3 computer models were included in the study. Nine patients, all with LBBB, underwent endocardial EAM (p1 to p9) during intrinsic rhythm, while 12 patients underwent epicardial EAM (p10 to p21) during both intrinsic rhythm and RV pacing. Three computer models (s1, s2, s3) were created based on patient-specific geometries obtained from patients p1, p2, and p3. Detailed information on individual patients and computer simulations is provided in Table 1 and 2, respectively.

Regional voltage differences in patients with LBBB

Regional unipolar and bipolar voltage differences were evaluated for the 9 patients who underwent endocardial EAM during intrinsic rhythm, as these patients had a high number of mapped points covering all segments of the LV.

Mean unipolar voltage amplitudes were approximately 4.5 mV (varying between 4.4-4.7 mV, ~33%) smaller in the septum compared to anterior, lateral and inferior within each endocardially mapped patient and for all 9 patients together (anterior: 13.5±5.6, lateral: 13.8±4.8, inferior: 13.5±6.1, septum: 9.1±4.5 mV, $p<0.001$). Regional unipolar voltage distributions in individual patients and representative voltage maps are provided in Figure 1. In contrast, bipolar voltage amplitudes were more heterogeneously distributed among the LV segments (anterior: 4.8±3.6, lateral: 5.0±3.1, inferior: 5.5±3.8, septum: 4.7±4.5 mV, $p<0.001$).

Regional voltage differences in simulations with LBBB and normal activation

Regional endocardial unipolar voltage differences were additionally assessed in three computer models. In all computer models, unipolar voltage amplitudes during an LBBB activation sequence were on average 4.0 mV (~24%) smaller in the septum and inferior compared to other LV segments (anterior: 16.7±3.8, lateral: 17.3±3.2, inferior: 13.1±3.7, septum: 13.1±4 mV). After inducing a normal synchronous activation sequence in the 3 computer models, regional unipolar voltage distributions became more uniform (Figure 2), and unipolar voltage amplitudes were on average similar between the segments (anterior: 14.1±3.4, lateral: 14.4±3.9, inferior: 13.7±4.4, and septal: 13.2±4.1 mV).

RV pacing induced voltage differences in patients

An overview of pacing-induced voltage changes for patients and computer models is provided in Figure 3. Pacing-induced unipolar voltage changes were analyzed in the 12 patients who underwent epicardial EAM (Figure 4). Overall, unipolar voltage during RV pacing did not differ significantly from the value during intrinsic conduction (intrinsic: 7.8±5.0, RV paced: 8.0±6.9 mV, $p=0.709$), but RV pacing caused considerable changes in these voltage amplitudes (IQR: 53% of intrinsic value; Figure 3). The absolute change in unipolar voltage amplitude between intrinsic rhythm and RV pacing was substantial: 3.6±5.9 mV (52±110% of intrinsic value). Larger unipolar voltage changes were present in electrograms with a larger amplitude during intrinsic rhythm (Bland-Altman analysis in Figure 4C).

RV and LV pacing-induced voltage differences in computer models

Pacing-induced unipolar voltage differences (Figure 3) at the epicardium and endocardium were additionally evaluated in computer models (Figure 5 and 6 respectively). Similar to the patient data, the direction of pacing-induced unipolar voltage changes could be either positive or negative and larger differences were present in electrograms with larger voltage amplitudes during intrinsic rhythm (Bland-Altman analyses in Figure 5C and 6C). Overall there was a positive correlation between the mean- and absolute unipolar voltage differences (from the Bland-Altman plots in Figure 5C and 6C) for both endocardial and epicardial unipolar voltage amplitudes (R: 0.1477-0.3881, p-values<0.001).

Mean epicardial unipolar voltage was distinct for different activation sequences (intrinsic: 17.4±5.9, RV pacing: 18.7±8.3, and LV pacing: 19.6±6.4 mV; Figure 5A), with the greatest change in unipolar voltage difference occurring during LV pacing (IQR: 63 and 40 for epicardium and endocardium respectively; Figure 3). The absolute mean difference between intrinsic epicardial unipolar voltage and pacing was 6.0±5.9 (40±53% of intrinsic value) for RV pacing and 6.2±5.3 mV (45±56% of intrinsic value) for LV pacing.

Mean endocardial unipolar voltage amplitudes were also affected by changing activation sequence (intrinsic: 13.7±4.3, RV pacing: 14.0±4.7, and LV pacing: 12.7±4.7 mV; Figure 6A), although these differences were much smaller than the epicardial values (Figure 3). The mean absolute difference between intrinsic endocardial unipolar voltage and pacing was 3.3±3.2 (28±33% of intrinsic value) for RV pacing and 3.8±3.2 mV (30±30% of intrinsic value) for LV pacing.

Discussion

This is the first study elucidating the voltage distribution during an LBBB activation sequence and investigating pacing-induced voltage changes in patients with possible explanations provided by computer simulations. We demonstrated that an LBBB activation sequence, in absence of scar, is associated with lower unipolar voltage amplitudes in the septum. We furthermore showed, using computer modelling, that these LBBB-associated low septal unipolar voltage amplitudes are functional, because they completely abolished during a normal synchronous activation sequence. Furthermore, modifying the activation sequence by ventricular pacing substantially changed unipolar voltage amplitudes in patients and computer models.

Together these results strongly indicate that activation sequence is a major determinant of local unipolar voltage amplitude and that the low septal voltage amplitudes in LBBB hearts can be explained exclusively by the specific activation sequence.

The septum: a challenging myocardial region

In our data, endocardial EAM LBBB patients demonstrated smaller unipolar voltage amplitudes in the septum compared to other LV segments. This difference was substantial (average 4.5 mV [~33%] lower) and present in every single patient. More interesting, these regional unipolar voltage amplitudes differences disappeared after restoring a normal activation sequence in the computer models, indicating that these low septal voltage amplitudes are exclusively due to an LBBB activation sequence, as geometrical and tissue properties were kept constant in the model. Low septal unipolar voltage amplitudes have not previously been associated with an LBBB activation sequence, although substantial regional variation in septal voltage amplitudes have been reported by Tung et al.[8].

Detailed EAM studies by Auricchio et al. showed that an LBBB activation sequence is characterized by a slow impulse conduction originating from the RV free wall gradually propagating to the LV lateral wall.[9] Long transseptal times, typically >30 ms, were also demonstrated by endocardial mapping in LBBB patients[18] and in canine LBBB hearts[19]. A long transseptal time reflects an electrical separation between the RV and LV and slow transseptal conduction. The slow conduction across the septum during LBBB activation may be explained by an activation sequence propagating perpendicular to the fiber orientation. Propagation velocity perpendicular to the fiber orientation is half of that along the fiber direction.[20] Interestingly, LBBB even in the absence of reduced LV function already causes regional changes in conduction velocity by lateralization of connexin43.[21] Thus, low septal unipolar voltage amplitudes (in the absence of scar) during LBBB activation sequences may be partially explained by slow conduction across the septum.

Pacing-induced voltage changes

The substantial pacing-induced voltage amplitude changes in the LV free wall support the idea that activation sequence created low voltage amplitudes are not a specific property of the septum. Moreover, because during RV pacing there is a

whole range of activation sequences within the LV free wall, also a wide range of changes (both increases and decreases) were observed. Clearly, these changes were substantial and more variable at the epicardium (mean absolute difference: 3.6-6.2 mV corresponding to 40-53% of intrinsic value; IQR differences: 53-63% of intrinsic value) compared to the endocardium (mean absolute difference: 3.3-3.8 mV corresponding to 28-30% of intrinsic value; IQR differences: 37-40% of intrinsic value). Therefore, in using voltage maps for scar delineation, activation sequence needs to be taken into account.[8]

The fact that we observe these wavefront dependencies of unipolar voltage amplitudes may be surprising, because they are considered to have a larger field of view compared to bipolar measurements. Several studies already investigated pacing-induced voltage changes, but these focused solely on bipolar measurements.[22,23] Blauer et al. confirmed in a bidomain model that different catheter inclination angles substantially impact the accuracy of identifying lesions by bipolar mapping.[23] Brunckhorst et al.[22] demonstrated in 11 ventricular tachycardia (VT) patients that RV pacing produced a >50% change in bipolar voltage at 28% sites and >100% at 10% sites. Therefore, it appears that, the range of fractional differences induced by activation sequence is similar for unipolar and bipolar voltage measurements.

Pacing-induced changes in unipolar voltage amplitudes have been investigated in two studies to date. Tung et al.[8] investigated the influence of changing wavefront on scar characterization (by low unipolar and bipolar recordings) in 29 VT patients. A variability of 22% for bipolar and 14% for unipolar voltage characterization of scar was observed with different activation sequences. Amorós-Figueras et al.[24] analysed voltage amplitude changes during intrinsic rhythm and RV pacing. In healthy myocardium, the IQR of change was 31% for endocardial unipolar voltage amplitudes, remarkably close to the IQR change of 37% that we observed after RV pacing in the computer models at the endocardium.

Clinical implications

To date, unipolar and bipolar voltage mapping are commonly used methods in clinical practice for invasive scar delineation.[1] In this study, we demonstrate that unipolar voltage amplitudes can be affected by different activation sequences and changes up to half of the intrinsic value are common. Furthermore, lower unipolar

voltage amplitudes are present in the septum in patients with a LBBB activation sequence.

These findings advocate for additional methods of invasive scar delineation. One potential method would be integration of DE-CMR data into the EAM system.[25] Alternative novel approaches for more accurate invasive scar delineation include the use of impedance measurements[24] and the wavefront-independent omnipolar electrograms.[26,27]

Study limitations

The study included both endocardially and epicardially mapped patients, which possibly affected voltage amplitudes. As such, this study focusses on relative voltage differences rather than absolute values. Moreover, we connected the two patient populations by using computer simulations from which we could extract both endocardial and epicardial data, covering the entire spectrum of patient data.

The present study primarily investigates unipolar voltage amplitudes and therefore additional studies are necessary to investigate the influence of activation sequence on bipolar voltage amplitudes.

Conclusion

This study demonstrates that an LBBB activation sequence in patients is associated with ~33% lower unipolar voltage amplitudes in the septum, and that these regional voltage amplitude differences resolve once a normal activation sequence is restored in a computer simulation. We additionally demonstrated that pacing-induced changes in the activation sequence substantially affect unipolar voltage amplitudes by ~30-50% of intrinsic value, particularly at the epicardium, while the direction of change can be both positive or negative. These findings are relevant for interpretation of voltage maps.

Funding

This work was granted access to HPC resources of CEA-TGCC under GENCI allocation x2016037379 and was supported by grants from the Swiss National Science Foundation under project 32003B_165802, from the Swiss Heart

Foundation, and by a restricted grant of Biologic Delivery Systems, Division of Biosense Webster a Johnson & Johnson Company.
The authors gratefully acknowledge financial support by Fondazione Cardiocentro Ticino, the Theo Rossi di Montelera Foundation, the Mantegazza Foundation, and FIDINAM to the Center of Computational Medicine in Cardiology. UCN received a Kootstra Talent Fellowship research grant from Maastricht University and was additionally funded by a research grant from the Dutch Heart Foundation (grant #2015T61). The funders had no role in study design, data collection and analysis, decision to publish or preparation of the manuscript.

Financial disclosures

FWP has received research grants from Medtronic, St. Jude Medical, LivaNova, Biosense Webster, MSD, and Biotronik. AA has been a consultant to Medtronic, Boston Scientific, LivaNova and Abbott, and has received speakers' fees from Medtronic, Boston Scientific and LivaNova. FR received speaker fees from Abbott and Bayer. KV received research grants from Medtronic and Abbott. The authors declare that no competing interests exist.

References

1. Priori SG, Blomstrom-Lundqvist C, Mazzanti A, et al. 2015 ESC Guidelines for the management of patients with ventricular arrhythmias and the prevention of sudden cardiac death: The Task Force for the Management of Patients with Ventricular Arrhythmias and the Prevention of Sudden Cardiac Death of the European Society of Cardiology (ESC)Endorsed by: Association for European Paediatric and Congenital Cardiology (AEPC). Europace 2015;17:1601-87.
2. Hutchinson MD, Gerstenfeld EP, Desjardins B, et al. Endocardial unipolar voltage mapping to detect epicardial ventricular tachycardia substrate in patients with nonischemic left ventricular cardiomyopathy. Circ Arrhythm Electrophysiol 2011;4:49-55.
3. Nguyen UC, Maffessanti F, Mafi-Rad M, et al. Evaluation of the use of unipolar voltage amplitudes for detection of myocardial scar assessed by cardiac magnetic resonance imaging in heart failure patients. PLoS One 2017;12:e0180637.
4. Codreanu A, Odille F, Aliot E, et al. Electroanatomic characterization of post-infarct scars comparison with 3-dimensional myocardial scar reconstruction based on magnetic resonance imaging. J Am Coll Cardiol 2008;52:839-42.
5. Wijnmaalen AP, van der Geest RJ, van Huls van Taxis CF, et al. Head-to-head comparison of contrast-enhanced magnetic resonance imaging and electroanatomical voltage mapping to assess post-infarct scar characteristics in patients with ventricular tachycardias: real-time image integration and reversed registration. European heart journal 2011;32:104-14.
6. Glashan CA, Androulakis AFA, Tao Q, et al. Whole human heart histology to validate electroanatomical voltage mapping in patients with non-ischaemic cardiomyopathy and ventricular tachycardia. European heart journal 2018 Epub Ahead of Print.
7. Josephson ME, Anter E. Substrate Mapping for Ventricular Tachycardia: Assumptions and Misconceptions. JACC: Clinical Electrophysiology 2015;1:341-52.
8. Tung R, Josephson ME, Bradfield JS, Shivkumar K. Directional Influences of Ventricular Activation on Myocardial Scar Characterization: Voltage Mapping With Multiple Wavefronts During Ventricular Tachycardia Ablation. Circ Arrhythm Electrophysiol 2016;9.
9. Auricchio A, Fantoni C, Regoli F, et al. Characterization of left ventricular activation in patients with heart failure and left bundle-branch block. Circulation 2004;109:1133-9.
10. Mafi Rad M, Blaauw Y, Dinh T, et al. Different regions of latest electrical activation during left bundle-branch block and right ventricular pacing in cardiac resynchronization therapy patients determined by coronary venous electro-anatomic mapping. Eur J Heart Fail 2014;16:1214-22.
11. Potse M, Krause D, Kroon W, et al. Patient-specific modelling of cardiac electrophysiology in heart-failure patients. Europace 2014;16 Suppl 4:iv56-iv61.
12. Nguyen UC, Potse M, Regoli F, et al. An in-silico analysis of the effect of heart position and orientation on the ECG morphology and vectorcardiogram parameters in patients with heart failure and intraventricular conduction defects. J Electrocardiol 2015;48:617-25.
13. Krause D, Potse M, Dickopf T, Krause R, Auricchio A, Prinzen F. Hybrid Parallelization of a Large-Scale Heart Model. In: Rainer Keller, David Kremer, Jan-Phillip Weiss, editors: Facing the Multicore - Challenge II; Aspects of New Paradigms

and Technologies in Parallel Computing. Lecture Notes in Computer Science, Volume 7174, 2012.
14. Potse M, Dube B, Richer J, Vinet A, Gulrajani RM. A comparison of monodomain and bidomain reaction-diffusion models for action potential propagation in the human heart. IEEE Trans Biomed Eng 2006;53:2425-35.
15. ten Tusscher KH, Noble D, Noble PJ, Panfilov AV. A model for human ventricular tissue. Am J Physiol Heart Circ Physiol 2004;286:H1573-89.
16. Potse M, Dube B, Vinet A. Cardiac anisotropy in boundary-element models for the electrocardiogram. Med Biol Eng Comput 2009;47:719-29.
17. White J, Rassweiler A, Samhouri J, Stier A, White C. Ecologists should not use statistical significance tests to interpret simulation model results. Oikos 2014;123: 385–388.
18. Prinzen FW, Auricchio A. Is echocardiographic assessment of dyssynchrony useful to select candidates for cardiac resynchronization therapy? Echocardiography is not useful before cardiac resynchronization therapy if QRS duration is available. Circ Cardiovasc Imaging 2008;1:70-7; discussion 8.
19. Strik M, van Deursen CJ, van Middendorp LB, et al. Transseptal conduction as an important determinant for cardiac resynchronization therapy, as revealed by extensive electrical mapping in the dyssynchronous canine heart. Circ Arrhythm Electrophysiol 2013;6:682-9.
20. Spach MS, Miller WT, 3rd, Geselowitz DB, Barr RC, Kootsey JM, Johnson EA. The discontinuous nature of propagation in normal canine cardiac muscle. Evidence for recurrent discontinuities of intracellular resistance that affect the membrane currents. Circ Res 1981;48:39-54.
21. Spragg DD, Akar FG, Helm RH, Tunin RS, Tomaselli GF, Kass DA. Abnormal conduction and repolarization in late-activated myocardium of dyssynchronously contracting hearts. Cardiovasc Res 2005;67:77-86.
22. Brunckhorst CB, Delacretaz E, Soejima K, Maisel WH, Friedman PL, Stevenson WG. Impact of changing activation sequence on bipolar electrogram amplitude for voltage mapping of left ventricular infarcts causing ventricular tachycardia. Journal of interventional cardiac electrophysiology : an international journal of arrhythmias and pacing 2005;12:137-41.
23. Blauer JJ, Swenson D, Higuchi K, et al. Sensitivity and specificity of substrate mapping: an in silico framework for the evaluation of electroanatomical substrate mapping strategies. J Cardiovasc Electrophysiol 2014;25:774-80.
24. Amoros-Figueras G, Jorge E, Alonso-Martin C, et al. Endocardial infarct scar recognition by myocardial electrical impedance is not influenced by changes in cardiac activation sequence. Heart Rhythm 2017.
25. Nguyen UC, Mafi-Rad M, Aben JP, et al. A novel approach for left ventricular lead placement in cardiac resynchronization therapy: Intraprocedural integration of coronary venous electroanatomic mapping with delayed enhancement cardiac magnetic resonance imaging. Heart Rhythm 2017;14:110-9.
26. Deno DC, Balachandran R, Morgan D, Ahmad F, Masse S, Nanthakumar K. Orientation-Independent Catheter-Based Characterization of Myocardial Activation. IEEE Trans Biomed Eng 2017;64:1067-77.
27. Masse S, Magtibay K, Jackson N, et al. Resolving Myocardial Activation With Novel Omnipolar Electrograms. Circ Arrhythm Electrophysiol 2016;9:e004107.

Table 1

Patient characteristics

Patient	Age	Sex	BMI (m^2/kg)	LVEF (%)	Type	NYHA	Conduction	QRSd (ms)	Wavefronts	Mapping	Nr of EGMs
p1	73	F	30	39	NCMP	3	LBBB	139	Intrinsic	LV endo	167
p2	70	M	23	35	ICMP	2	LBBB	179	Intrinsic	LV endo	88
p3	54	M	32	34	ICMP	2	LBBB	165	Intrinsic	LV endo	131
p4	70	M	24	21	NCMP	2	LBBB	160	Intrinsic	LV endo	206
p5	69	F	30	17	ICMP	3	LBBB	185	Intrinsic	LV endo	199
p6	69	F	31	35	ICMP	3	LBBB	156	Intrinsic	LV endo	236
p7	69	M	26	45	NCMP	2	LBBB	154	Intrinsic	LV endo	163
p8	85	M	31	32	NCMP	3	LBBB	180	Intrinsic	LV endo	244
p9	69	M	24	28	ICMP	2	LBBB	170	Intrinsic	LV endo	159
p10	75	M	27	34	NCMP	2	LBBB	142	Intrinsic/RV	LV epi (veins)	50
p11	80	M	26	29	ICMP	2	IVCD	136	Intrinsic/RV	LV epi (veins)	26
p12	42	F	31	28	NCMP	2	LBBB	160	Intrinsic/RV	LV epi (veins)	27
p13	75	F	23	15	NCMP	3	LBBB	122	Intrinsic/RV	LV epi (veins)	47
p14	71	F	26	29	NCMP	2	LBBB	156	Intrinsic/RV	LV epi (veins)	41
p15	65	F	27	10	NCMP	3	LBBB	150	Intrinsic/RV	LV epi (veins)	41
p16	52	M	34	24	NCMP	3	LBBB	136	Intrinsic/RV	LV epi (veins)	19
p17	57	F	25	26	NCMP	2	IVCD	158	Intrinsic/RV	LV epi (veins)	34
p18	60	F	26	20	NCMP	2	LBBB	132	Intrinsic/RV	LV epi (veins)	42
p19	61	M	21	32	NCMP	2	LBBB	154	Intrinsic/RV	LV epi (veins)	48
p20	58	M	28	26	NCMP	3	LBBB	150	Intrinsic/RV	LV epi (veins)	13
p21	80	M	25	24	NCMP	3	LBBB	156	Intrinsic/RV	LV epi (veins)	29

BMI=body-mass-index, ICMP=ischemic cardiomyopathy, EGMs=electrograms, F=female, IVCD=intraventricular conduction defect, LBBB=left bundle branch block, LV=left ventricle, LVEF=LV ejection fraction, M=male, NCMP=non-ischemic CMP, NYHA=New York Heart Association functional class, QRSd=QRS duration, RV=right ventricle.

Table 2

Computer model characteristics

Model	Fitted to patient	Conduction	Wavefronts	Mapping	Nr of EGMs (endo/epi)
s1	p1	LBBB/normal	Intrinsic/RV/LV	LV endo/epi	4105/4540
s2	p2	LBBB/normal	Intrinsic/RV/LV	LV endo/epi	6732/6810
s3	p3	LBBB/normal	Intrinsic/RV/LV	LV endo/epi	5626/6574

LV=left ventricle, LBBB=left bundle branch block, RV=right ventricle.

Figure 1

Regional differences on endocardial voltage amplitudes in patients with LBBB.

(A) Mean±SD of endocardial unipolar voltage amplitudes per patient grouped according to location. Lower unipolar voltage amplitudes are consistently present in the septum. * indicates p ≤0.001 based on Kruskall-Wallis test. (B) Endocardial voltage maps of 2 representative patients with LBBB. UnipV = unipolar voltage amplitude.

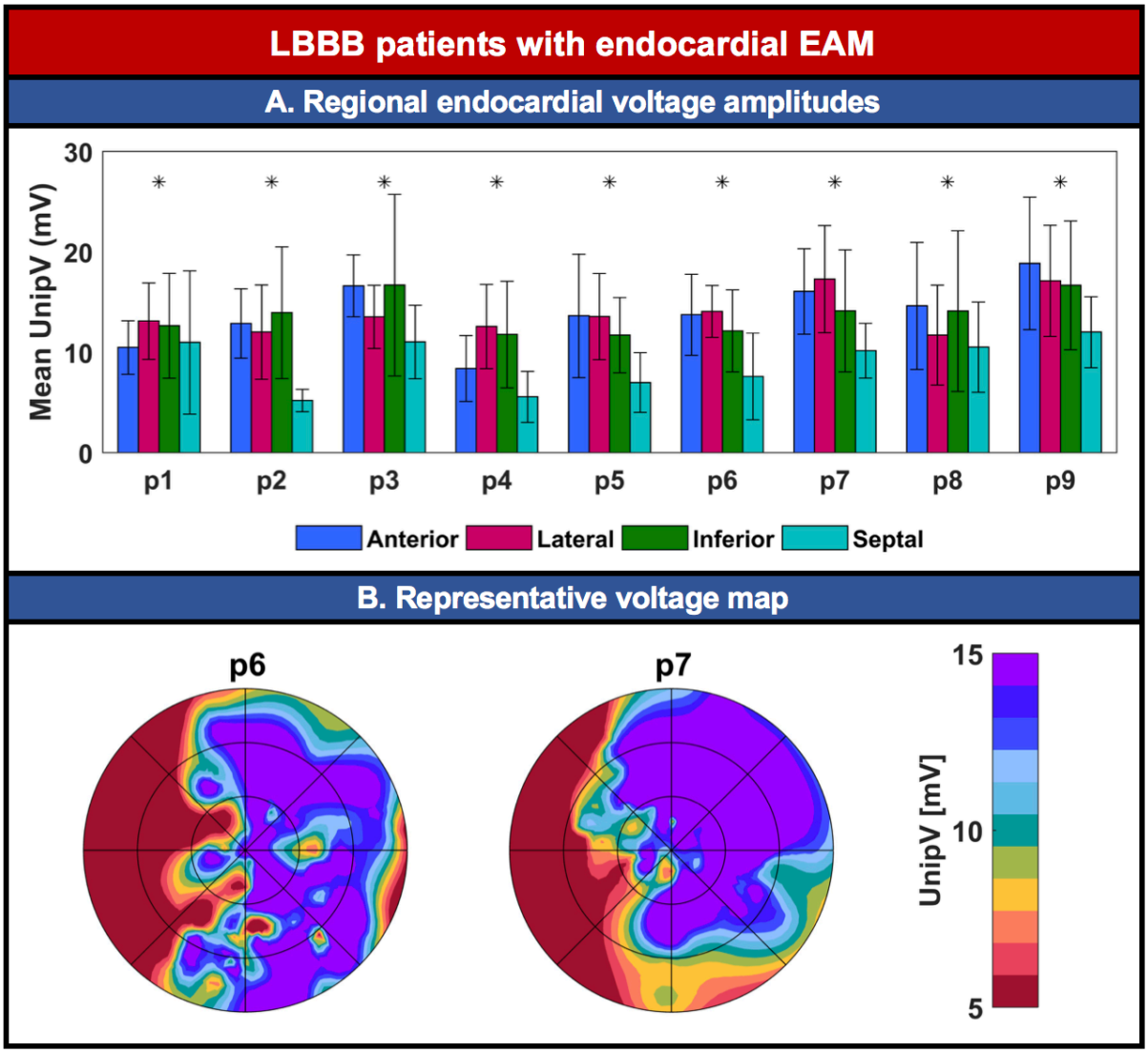

Figure 2

Regional differences in endocardial voltage amplitudes in a computer model. Activation (left) and voltage (middle) maps with accompanying location bar graphs (right) of simulations s2 during an LBBB (top panels) and normal (bottom panels) activation sequence. Unipolar voltage amplitudes are smaller in the septum and inferior during LBBB. These lower voltage amplitudes disappear when a normal activation sequence is restored. UnipV = unipolar voltage amplitude.

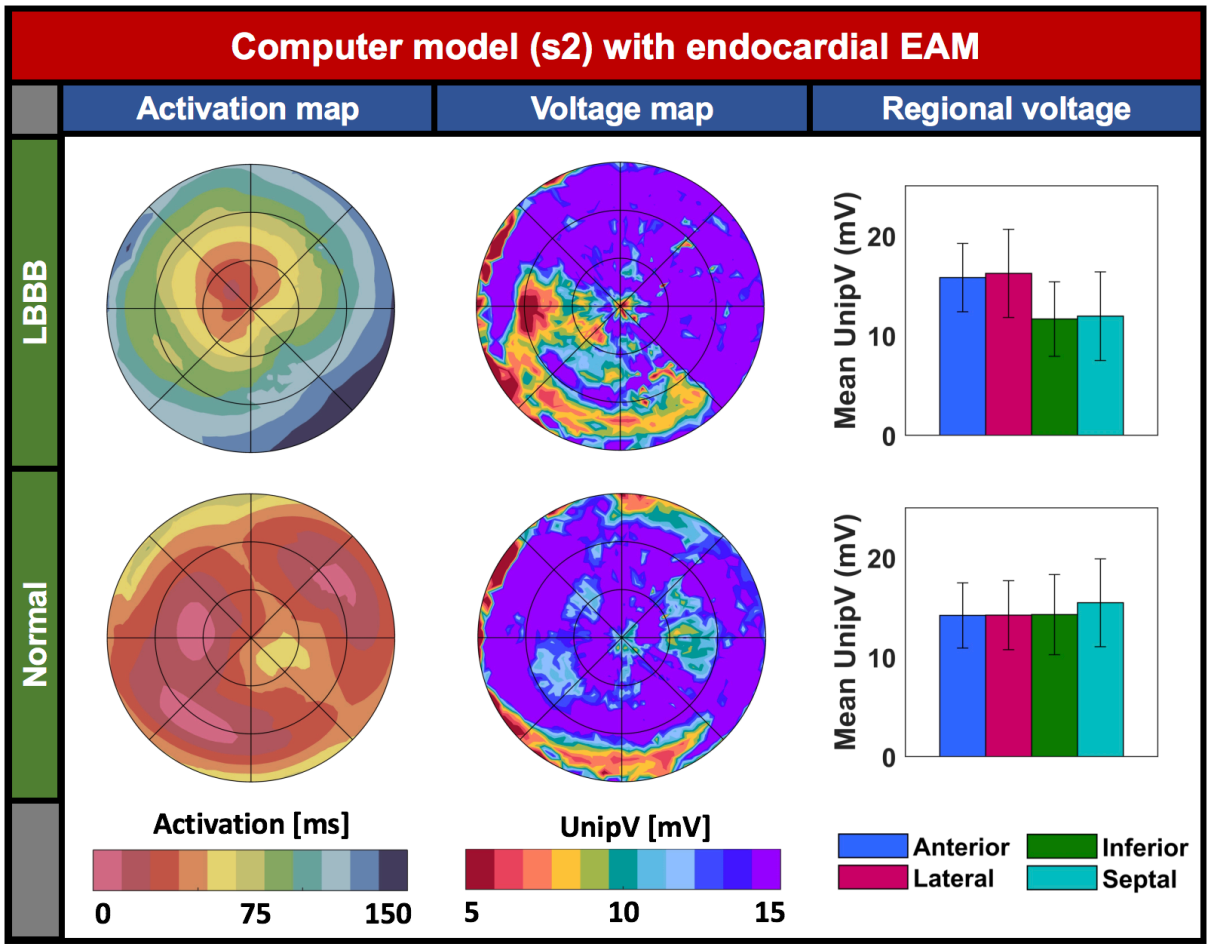

Figure 3

Overview of differences in voltage amplitude values after changing the sequence of activation by pacing.

Differences are depicted in percentage of intrinsic value. The red boxplots indicate the differences induced by RV pacing, while the green boxplots indicate the LV pacing-induced changes. The central mark in the box indicates the median, and the bottom and top edges of the box indicate the 25th and 75th percentiles, respectively. The whiskers extend to the most extreme data points not considered outliers. Changes are grouped for epicardial EAM patients (*n*=9) and computer simulations (*n*=3) with both endocardial and epicardial EAM points.

The IQR of RV pacing-induced changes of patients with epicardial EAM is very similar to the changes observed at the epicardium in the computer models. The IQR of unipolar voltage changes is generally larger for the epicardium compared to the endocardium and higher after LV pacing compared to RV pacing. UnipV = unipolar voltage amplitude.

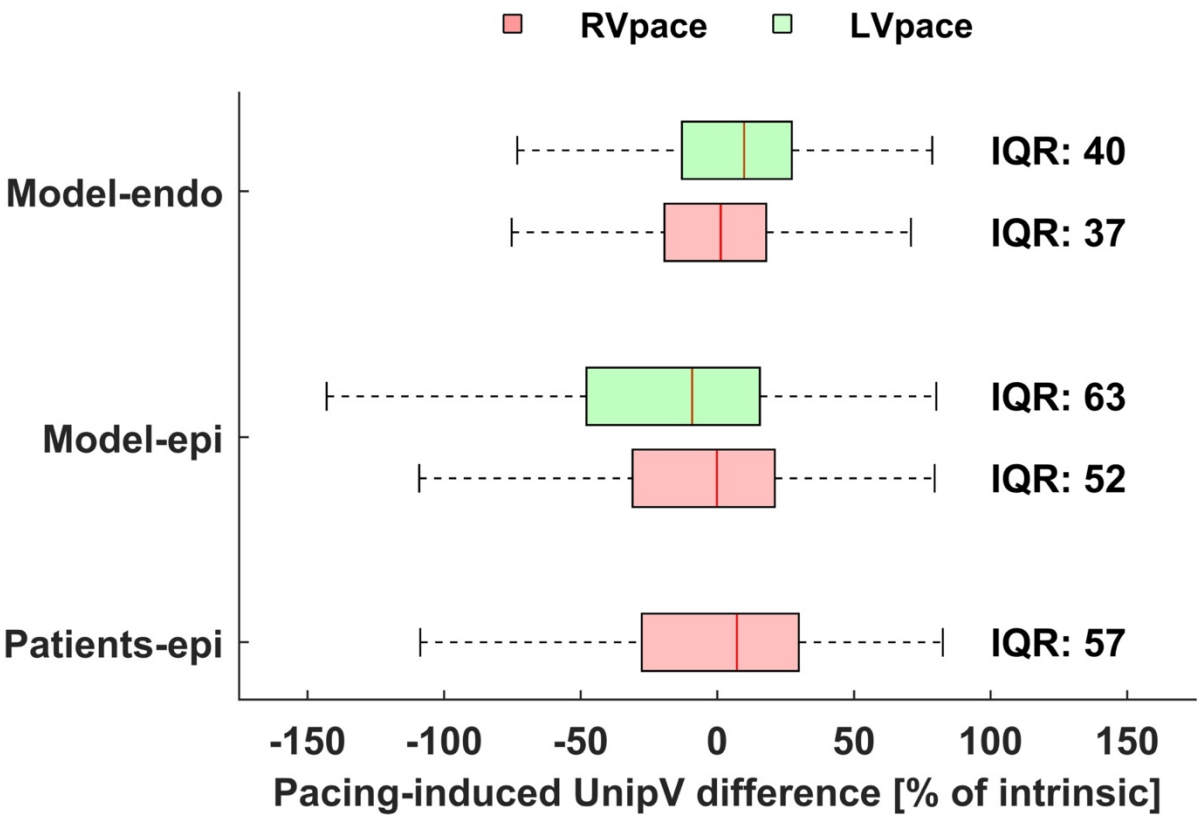

Figure 4

Pacing-induced voltage changes at the epicardium in patients.

(A) Mean±SD of endocardial unipolar voltage amplitudes per patient during intrinsic rhythm and RV pacing. * indicates p ≤0.05 based on Mann Whitney u-test. (B) Epicardial (coronary venous) voltage map of a representative patient (p19) during intrinsic rhythm and RV pacing. The mean voltage amplitude does not change much, but substantial changes per electrogram are present. (C) Bland-Altman analyses for voltage amplitudes differences between intrinsic rhythm and RV pacing. RV pacing induces substantial changes in voltage amplitudes, although the direction of change varies. The larger the voltage amplitude during intrinsic rhythm, the larger the change after pacing. UnipV = unipolar voltage amplitude.

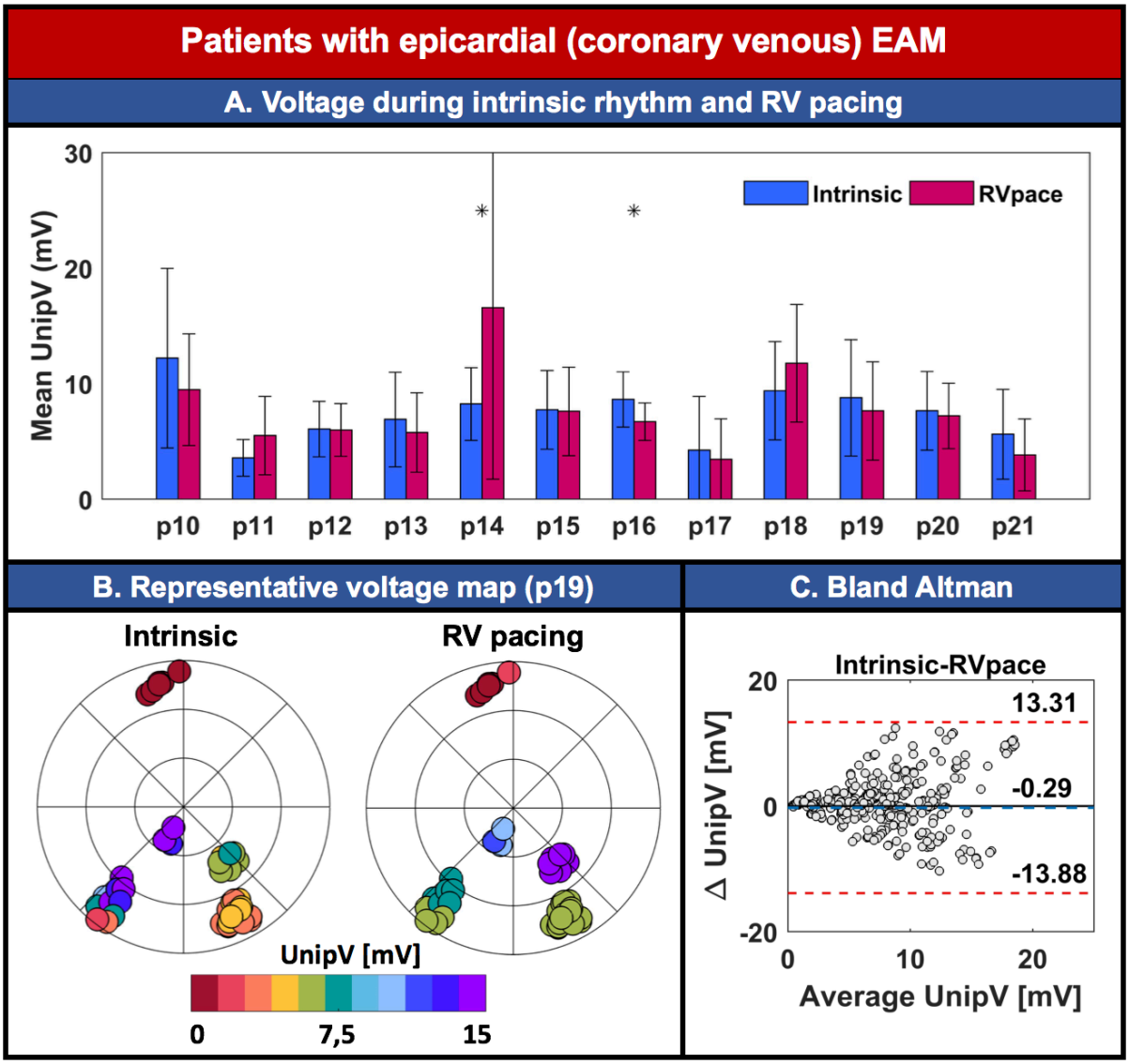

Figure 5

Pacing-induced voltage changes at the epicardium in computer models.

(A) Epicardial unipolar voltage maps of computer simulation s1 during different activation sequences induced by pacing. The septal quarters are displayed in white as the epicardium does not contain septum. (B) Mean unipolar voltage amplitudes for every computer model during different activation sequences. (C) Bland-Altman analyses comparing the difference between intrinsic (LBBB) and paced unipolar voltage amplitudes. Similarly, like the clinical data, the mean unipolar voltage amplitudes do not change much, but substantial point-by-point changes are observed. UnipV = unipolar voltage amplitude.

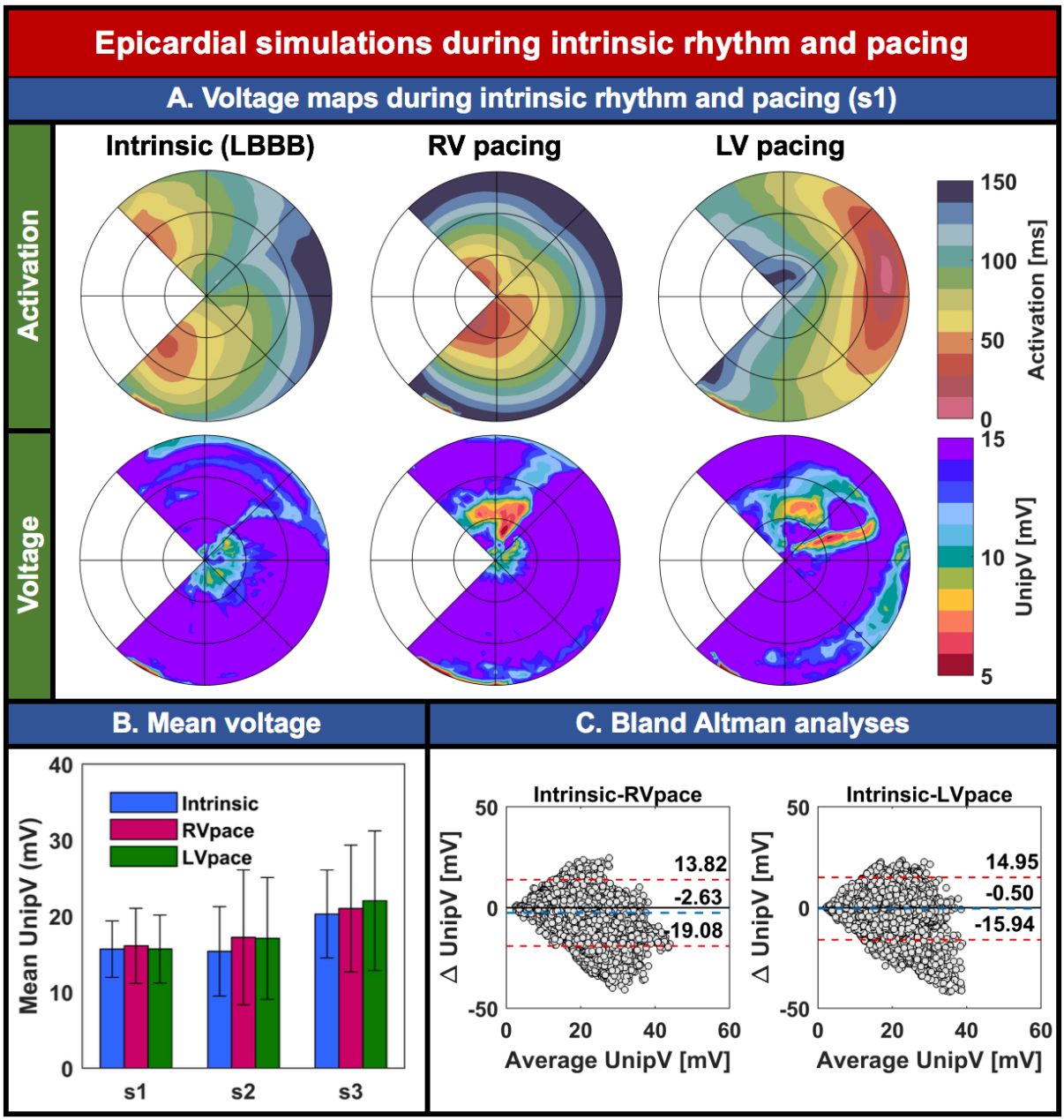

Figure 6

Pacing-induced voltage changes at the endocardium in computer models.

(A) Endocardial unipolar voltage maps of computer model s1 during different activation sequences induced by pacing. (B) Mean unipolar voltage for every computer model during different activation sequences. (C) Bland-Altman analyses comparing the difference between intrinsic (LBBB) and paced unipolar voltage amplitudes. UnipV = unipolar voltage amplitude.